Hydrol. Earth Syst. Sci. Discuss., https://doi.org/10.5194/hess-2018-234
Manuscript under review for journal Hydrol. Earth Syst. Sci.
Discussion started: 14 May 2018

Hydrology and Earth System Sciences Discussions
Open Access

Seasonal variability in evapotranspiration partitioning and its relationship with crop development and water use efficiency of winter wheat

Ying Ma[1], Praveen Kumar[2], and Xianfang Song[1]

[1]Key Laboratory of Water Cycle and Related Land Surface Processes, Institute of Geographic Sciences and Natural Resources Research, Chinese Academy of Sciences, Beijing 100101, China

[2]Department of Civil and Environmental Engineering, University of Illinois at Urbana-Champaign, Urbana 61801, IL, USA

Corresponding to: Ying Ma (maying@igsnrr.ac.cn)

Abstract

The partitioning of evapotranspiration (ET) into soil evaporation (E) and crop transpiration (T) is fundamental for accurately monitoring agro-hydrological processes, assessing crop productivity, and optimizing water management practices. In this study, the isotope tracing technique was used to partition ET and quantify the root water uptake sources of winter wheat during the 2014 and 2015 growing seasons in Beijing, China. The correlations between seasonal ET partitioning and the leaf area index (LAI), grain yield, and water use efficiency (WUE) were investigated. The fraction of T in ET (F_T) between the greening and harvest

Hydrol. Earth Syst. Sci. Discuss., https://doi.org/10.5194/hess-2018-234
Manuscript under review for journal Hydrol. Earth Syst. Sci.
Discussion started: 14 May 2018

seasons was 0.82 on average and did not vary significantly among the different irrigation and fertilization treatments ($p > 0.05$). However, the values of F_T during the individual growth periods were remarkably distinct (ranging from 0.51 to 0.98) among the treatments. The seasonal variability in F_T could be effectively explained via a power-law function of the LAI ($F_T = 0.61\ \mathrm{LAI}^{0.21}$, $R^2 = 0.66$, $p < 0.01$). There was no significant relationship between F_T and the grain yield or WUE ($p > 0.05$). The total T during the jointing-heading and heading-filling periods (T_{jf}) had significantly quadratic relationships with the crop yield and WUE ($p < 0.01$). Both the crop yield and the WUE had high values under the T_{jf} range of 117.5-155.8 mm. Furthermore, the WUE was improved by increasing the ratio of E in ET (F_E) during the greening-jointing period and by reducing F_E during the filling-harvest period. Winter wheat mainly utilized soil water from the 0-20 cm (67.0%), 20-70 cm (42.0%), 0-20 cm (38.7%), and 20-70 cm (34.9%) layers during the greening-jointing, jointing-heading, heading-filling, and filling-harvest periods, respectively. This indicated that the irrigation wetting layer should be controlled at depth of 70 cm to conserve water.

1 Introduction

Evapotranspiration (ET) represents a critical component of the water cycle in the soil-plant-atmosphere continuum (SPAC), which is fundamental for crop development and for determining water use efficiency (WUE). Partitioning ET into soil evaporation (E) and plant transpiration (T) can provide deep insight into an evaluation of the water saving potential and optimization of agro-management practices (Newman et al., 2006; Guan and Wilson, 2009; Agam et al., 2012). The majority of previous studies referred to T as the productive component of the crop yield, while E was described as the non-productive water loss (Agam et al., 2012; Van Halsema and Vincent, 2012; Ding et al., 2017). A positive linear function has generally been used to describe the relationship between the yield and T provided that water was the main limiting factor on the yield (Hanks, 1983; Ben-Gal and Shani, 2002; Tolk and Howell, 2009). Nevertheless, some studies claimed that E might indirectly benefit the crop yield by creating a microclimate that is more favorable for crop growth and productivity (Stanhill, 1973; Tolk et al., 1995; Burt et al., 2005; Kustas and Agam, 2013). Therefore, further research is necessary to separate the E and T components of ET and investigate their interrelationships with crop development and the WUE.

The partitioning of ET has been studied using several methods and techniques (Kool et al., 2014; Sutanto et al., 2014; Sprenger et al., 2016). Conventional hydrometric methods employed various techniques to directly measure ET (e.g., the eddy covariance technique, micro Bowen ratio energy balance method, and the weighing lysimeter approach) in addition to E (via a micro-lysimeter) or T (using sap flow sensors) (Mitchell et al., 2009; Cavanaugh et al., 2011; Liu et al., 2002; Zhang et al., 2003; Sun et al., 2006). Simulation models such as the Shuttleworth-Wallace model, the Food and Agriculture Organization (FAO) dual crop coefficient model, the HYDRUS-1D model, and the hybrid dual-source model (TVET) have also been used to simultaneously calculate E and T (Li et al., 2010; Zhang et al., 2013; Ding et al., 2017; Sutanto et al, 2012; Guan and Wilson, 2009). Since various fractionation processes such as condensation and evaporation leave characteristic imprint on the isotopic composition of water, the stable water isotopes of ^{18}O and D are considered ideal (natural) tracers for separating E and T from ET and tracking water through the soil based on distinct

Hydrol. Earth Syst. Sci. Discuss., https://doi.org/10.5194/hess-2018-234
Manuscript under review for journal Hydrol. Earth Syst. Sci.
Discussion started: 14 May 2018

isotopic signatures of water fluxes (Brunel et al., 1997; Sprenger et al., 2016). Water isotopes are highly fractionated during E processes, causing the remaining soil water to become enriched in heavy isotopes; meanwhile, T does not modify the isotopic composition, since there is typically no isotopic fractionation during water uptake or transport through roots and stems (Wang et al., 2010a; Sutanto et al, 2014).

Due to recent advances in the techniques and instruments used to collect measurements of $\delta^{18}O$ and δD for both liquid water and water vapor, isotope-based methods have been increasingly applied to agricultural systems to precisely partition ET at different time scales (Wang et al., 2012; Wang and Yamanaka, 2014; Zhang et al., 2011; Wang et al., 2016; Lu et al., 2017; Wei et al., 2018). It was reported that T accounts for 20-80% of the total seasonal ET in sparse canopies and row crops, especially under arid and semi-arid conditions (Agam et al., 2012; Coenders-Gerrits et al., 2014; Kool et al., 2014; Lu et al., 2017). At the daily scale, the ratio of T within ET (F_T) varied over a wide range of 0.2-1 within a rice paddy field during a complete growing season in Mase, Tsukuba (Wei et al., 2015). The daily F_T also changed greatly (0.52-0.96) throughout the growing season of maize in northwestern China (Wen et al., 2016; Wu et al., 2017). Substantial differences in F_T were discovered between the late filling stage (0.83) and the stage of wax ripeness (0.6) in an irrigated field of winter wheat in the North China Plain (NCP) (Zhang et al., 2011). The values of F_T changed from 0.46 to 0.74 after an irrigation event during the early growth stage of winter wheat in the NCP and in central Morocco (Wang et al., 2012; Aouade et al., 2016). These studies revealed very distinct changes in F_T throughout the crop-growing season and the significant influence of irrigation on the partitioning of ET. It is therefore necessary to thoroughly clarify the seasonal variability in the partitioning of ET in association with its major influencing factors.

The seasonal variations in ET partitioning are strongly associated with crop development (Sprenger et al., 2016). The leaf area index (LAI) is often regarded as an effective crop parameter for explaining the variabilities in the E/ET ratio (F_E) and F_T. It is commonly believed that F_E decreases exponentially with the LAI for most crops and that the F_T increases logarithmically with an increase in the LAI in the absence of water stresses (Villalobos and Fereres, 1990; Liu et al., 2002; Yu et al., 2009; Kato et al., 2004). However, Kang et al. (2003) proposed that F_T and the LAI exhibited a saturation relationship for wheat and maize in a semi-arid region of Northwest China. Several recent studies identified a power-law correlation between F_T and the LAI for agricultural systems at both the global scale and in certain croplands (Wang et al., 2014; Wei et al., 2015; Wu et al., 2017; Lu et al., 2017; Zhao et al., 2018). In addition, numerous possibilities were suggested for high F_T even under low LAI conditions. To illustrate the global variability in the partitioning of ET, Wang et al. (2014) further developed a function relating F_T to the growth stage relative to the timing of the peak LAI. It was evident that the LAI within different growth stages should be utilized to evaluate the variability in ET partitioning and crop water use capabilities.

The ability of a crop to access water resources from different soil horizons can be estimated via the root water uptake (Asbjornsen et al., 2007; Wang et al., 2010b; Zhang et al., 2011; Yang et al., 2015). Common methods applied to assess water uptake patterns include the IsoSource model in addition to less than three-layer linear mixing models and Bayesian mixing models (Phillips and Gregg, 2003; McCole and Stern, 2007; Moore and Semmens, 2008; Stock and Semmens, 2013). The MixSIAR framework is the latest Bayesian stable isotope analysis mixing model in R that considers multiple sources of uncertainty and provides definite proportions of source contributions. It has been employed successfully to determine the contributions of soil water at different layers to the water uptake of summer maize (Ma and Song, 2016). The root water uptake also indicates the availability of soil water resources to crops, and it varies with different agricultural management practices. Therefore, combining the seasonal partitioning of ET with the development of the LAI and root water uptake patterns can provide a comprehensive understanding of E and T processes. It also help design a reasonable irrigation depth, which is vital for improving the crop yield and WUE in regions with a high food demand and limited water resources such as in the NCP.

The NCP constitutes one of the major food production regions in which winter wheat represents the main water-consuming crop. In addition, the NCP provides approximately 69% of the wheat production for all of China. However, irrigated agriculture practices throughout the NCP are facing critical challenges (i.e., very limited water supplies) to the provision of sufficient quantities of food. To optimize the irrigation strategies for winter wheat, considerable research has been conducted to determine the relationships among the seasonal ET with the crop yield and WUE (Li et al., 2005; Sun et al., 2006; Shang et al., 2006; Liu et al., 2013). E and T were also partitioned, and an exponential relationship between F_E and the LAI was established (Liu et al., 2002; Yu et al., 2009). Furthermore, E was reported to be an unproductive water loss, and thus, it should be reduced in regions with a severe water deficit. Recently, Zhang et al. (2011) simultaneously addressed the partitioning of ET and the characterization of root water uptake depths for winter wheat during the growing season.

Hydrol. Earth Syst. Sci. Discuss., https://doi.org/10.5194/hess-2018-234
Manuscript under review for journal Hydrol. Earth Syst. Sci.
Discussion started: 14 May 2018

However, the definite correlations between the magnitude and fraction of seasonal ET partitioning with the grain yield and WUE are still unclear. Further investigations are therefore required to demonstrate seasonal variations of ET partitioning and root water uptake pattern and quantify their relationships with the LAI, grain yield and WUE under different agricultural management practices.

In this study, the isotope mass balance approach was utilized in conjunction with the soil water balance method to partition the ET of winter wheat during the 2014 and 2015 growing seasons in Beijing, China. The three primary objectives of this study were to (1) detect the variations of ET partitioning during the different growth stages of winter wheat, (2) quantify the seasonal root water uptake patterns of winter wheat, and (3) determine the relationships between ET partitioning and the LAI, grain yield and WUE. The results were applied to establish optimal agricultural management practices and design the irrigation depth.

2 Materials and methods

2.1 Field experiments

Field experiments with winter wheat were conducted from 2013 to 2015 at the Irrigation Experiment Station of the China Institute of Water Resources and Hydropower Research (IWHR) at Daxing, Beijing (39°37′N latitude, 116°26′E longitude, 40.1 m a.s.l. elevation). The climate in this area is sub-humid with a mean annual precipitation of 540 mm, but only 20-30% of the precipitation occurs during the winter wheat season (Cai et al., 2009). The mean annual temperature is 12.1 ℃ and mean seasonal reference evapotranspiration (ET_0) of winter wheat is 610 mm. Soils in the 2-m profile were sampled every 20 cm depth to measure their physical and chemical properties. The depths with similar soil particle size and organic carbon were merged into one layer. The soil profile was finally divided into four layers and their main properties are shown in Table 1.

The winter wheat (variety: Zhongmai-175) was planted on October 9, 2013, and harvested on June 8, 2014, during the 2014 growing season. The sowing and harvest dates during the 2015 growing season were October 11, 2014, and June 8, 2015, respectively. Five irrigation and fertilization treatments (T1, T2, T3, T4, and T5) were applied from winter greening to the harvest season. Here, treatment T5 refers to the agricultural management practices employed by local farmers with a total irrigation of 240 mm and a nitrogen supply of 210 kg N ha^{-1} (as urea) (Table 2). In comparison with the reference treatment (T5), the T1 and T2 treatments had reduced irrigation of 60 mm from greening to jointing and 80 mm from the filling to the harvest period, respectively. The T3 and T4 treatments both reduced the irrigation during jointing-heading or heading-filling stage by 80 mm compared with treatment T5. The nitrogen (N) application rates for the T1 and T3 treatments were both 0.5-fold of that for treatment T5, while 1.5-fold of the nitrogen in treatment T5 was applied to both the T2 treatment and the T4 treatment. All the irrigation was provided in a single application per stage. The application date was 27 Mar, 22 Apr, and 22 May in 2014, while it was 29 Mar, 9 May, and 21 May in 2015, respectively. The detailed irrigation and fertilization schedules for these five treatments are shown in Table 2. Three replicates were conducted for every treatment in the plots with each area of 6 × 5 m. Basin irrigation with groundwater was implemented for all of the treatments. Precision-leveled basins were used to prevent runoff.

The soil water contents in the 2-m soil profile were measured at a 20-cm interval every 5-7 days in each plot using a TRIME-IPH probe based on the Time domain Reflectometry with Intelligent MicroElements technique (IMKO GmbH, Ettlingen, German). Additional measurements were conducted when soil water samples were collected for isotope analysis as well as before and after each irrigation or heavy rainfall event. Meanwhile, three plants in each plot were selected to manually observe their leaf areas (obtained by multiplying the leaf length and width), which were then calibrated using a leaf scanner (F915900, Canon, Canada). The LAI was calculated as the product of the calibrated leaf area per plant and the number of plants per unit area. The grain was air-dried, and the crop yield was recorded separately for each plot after harvesting.

Meteorological data including the precipitation, maximum and minimum air temperatures, solar radiation, wind speed and relative humidity were recorded every 30 min by the automatic weather station (Monitor Sensors, Caboolture QLD, Australia). The rainfall amounts were 77.0 mm and 74.7 mm between the greening and harvest seasons in 2014 and 2015, respectively. Both seasons were dry at 75% precipitation exceedance probabilities (PEPs) in terms of the rainfall frequencies during the last five decades in the Beijing area. However, there was an additional 34.8 mm of precipitation during the greening-jointing period and 26.9 mm less precipitation during the jointing-heading period in 2015 relative to 2014.

2.2 Water sampling and isotopic analyses

Different waters including the precipitation, irrigation water, soil water, and stem water were sampled to analyze the isotopic composition of ^{18}O and D. The precipitation was collected after each rainfall event via a rain collector coupled with a polyethylene bottle and funnel. A ping-pong ball was positioned at the funnel mouth (Wang et al., 2012). The ping-pong ball floated up when rain fell at the funnel mouth and enabled the rainfall to move into the bottle. Evaporation was then prevented during the rainfall process. The collected rainwater was transferred to a bottle immediately, sealed and stored. Irrigation water was sampled in each irrigation event.

Three stems of each treatment were sampled at an interval of about one week. Each stem was taken from the part between the soil surface and the first node of one representative plant. It was cut into pieces in 2-3 cm length, then put into a vial and sealed with parafilm. All the epidermises of the stems were removed to eliminate the effect of the isotopically depleted atmospheric water vapor on the stem water isotopic compositions (Brunel, 1997).

The soil water at depths of 10, 20, 30, 50, 70, 90, 110, 150, and 200 cm was sampled on and after the day of collecting stem water, and after each irrigation or heavy rainfall event. A suction lysimeter made of a Teflon pipe and porous ceramic cup was installed and used to abstract the soil water at each depth (Wang et al., 2012). If the soil water content was too low to collect soil water by the suction lysimeter, soil sample instead was collected using a hand auger.

All of the stem and soil samples were kept refrigerated (-15 ℃ to -20 ℃) prior to measuring the isotopic compositions. The cryogenic vacuum distillation system (LI-2000, LICA, Beijing, China) was applied to extract water in the soil and stem samples (West et al., 2006). The ratio of $^{2}H/^{1}H$ and $^{18}O/^{16}O$ of different water samples were measured on a Los Gatos Research (LGR) DLT-100 liquid water isotope analyzer (San Jose, CA, America). They were calibrated against the VSMOW international standards and converted to δD and $\delta^{18}O$ values. The measuring precision for δD and $\delta^{18}O$ was ±1‰ and ±0.1‰, respectively.

2.3 Evapotranspiration partitioning methods

Transpiration changes soil water content but keep soil water isotopic composition constant because water uptake from soil by plants does not result in isotopic fractionation (Zimmerman et al., 1967). On the contrary, both soil water content and soil water isotopic composition are changed in evaporation process (Allison and Barnes, 1983). Many previous studies reported that the water balance and isotope mass balance equations were robust to partition ET into E and T when sampling intervals were short (Hsieh et al., 1998; Robertson and Gazis, 2006; Wenninger et al., 2010; Wang et al., 2012). In this study, the ET in the day of the stem water sampling was partitioned into E and T using the following soil water balance and isotope mass balance equations in the 0-200 cm profile:

$$m_f - m_i = m_{\mathrm{P}} + m_{\mathrm{I}} - m_{\mathrm{ET}} - m_{\mathrm{D}} - m_{\mathrm{R}} \quad (1)$$

$$m_{\mathrm{ET}} = m_{\mathrm{E}} + m_{\mathrm{T}} \quad (2)$$

$$\delta_{\mathrm{E}} m_{\mathrm{E}} + \delta_{\mathrm{T}} m_{\mathrm{T}} = \delta_i m_i + \delta_{\mathrm{P}} m_{\mathrm{P}} + \delta_{\mathrm{I}} m_{\mathrm{I}} - \delta_f m_f - \delta_{\mathrm{D}} m_{\mathrm{D}} - \delta_{\mathrm{R}} m_{\mathrm{R}} \quad (3)$$

where m and δ represent the water flux and isotopic composition of δ^{18}O in different waters, respectively, f and i denote the final and initial state of the soil water storage in one sampling day of stem water, respectively, P is the precipitation, I is the irrigation, D is the drainage out of the soil profile, and R is the surface runoff. There were two or three times of stem water sampling during each growth period. The average value of the partitioned E or T during one growth period was used to represent the ET partitioning result in this period.

The final and initial soil water storage (m_f and m_i) in Eq. (1) was calculated using the measured depth-weighted volumetric soil water content. Meanwhile, the precipitation (m_{P}) was obtained from meteorological observations, while the irrigation (m_{I}) was artificially controlled and therefore measurable. The soil moisture near the bottom boundary remained steady and generally below the field capacity throughout the experimental seasons. Therefore, the amount of drainage (m_D) was neglected in this study. In addition, no runoff (m_R) was observed during the field experiments.

The values of δ_i and δ_f are the depth-weighted δ^{18}O averages for the whole soil profile collected on and after the day of stem water sampling, respectively, while δ_P and δ_I are the measured δ^{18}O values of the precipitation and irrigation, respectively. The δ^{18}O value of evaporation (δ_E) is estimated using the fraction factor $\alpha_{\text{liquid-vapor}} = (\delta_l + 1000)/ (\delta_v + 1000)$ (Wang et al., 2012). The evaporated water δ_v (δ_E in Eq. (3)) is assumed to be in isotopic equilibrium with the soil water δ_l (δ_i in Eq. (3)). The value of $\alpha_{\text{liquid-vapor}}$ is given as 1.0102 at an air temperature of 15 ℃ following Clark and Fritz (1997). As there is no fractionation in the T processes of winter wheat (Wang and Yakir, 2000), the value of δ_T is determined using the measured δ^{18}O of stem water.

2.4 MixSIAR model

The MixSIAR Bayesian mixing model (v2.1.3) incorporating with dual stable water isotopes (δD and δ^{18}O) was used to identify the water uptake sources of winter wheat. In field experiments, precipitation or irrigation water infiltrated and finally mixed into the old soil water. Groundwater could hardly contribute to crop water use (the average maximum rooting depth was 2 m for winter wheat) under the condition of the deep water table depth (mean of 16 m below the soil surface). It can be supposed that soil water at different depths was proportionally sourced by winter wheat. Four layers was divided as 0-20, 20-70, 70-150, and 150-200 cm depth along the 2-m soil profile in terms of their water isotopic compositions, soil moisture contents and root distributions. The dual stable isotopes of the soil water in each layer (raw source data) and of the stem water (mixture data) were input to the MixSIAR model to quantify the main root water uptake depth. The Markov chain Monte Carlo (MCMC) was used in the MixSIAR model for estimating the probability density functions of variables as the MCMC was advantageous to estimate the entire distribution for each variable. The MCMC parameter run length was set to "very long" to converge on the true posterior distribution for each variable. The model error was evaluated using the SIAR (process and residual). The estimated 5th, 25th, 50th, 75th, and 95th percentiles of the posterior contributions of each source described the distribution associated with the proportional contribution of each source to winter wheat. The 50% percentile represented the median source contribution value for each source.

2.5 Data analysis

The statistical analyses of the variation in each isotopic composition, soil moisture distribution, ET component and associated fraction, and root water uptake pattern during each season and treatment were all performed using a Statistical Package for the Social Sciences (SPSS) 19.0 software package. The WUE was defined as the ratio between the crop yield and the total ET from the greening to harvest season of winter wheat (Hussain et al., 1995). In this study, the highest WUE value without an evident decrease in the grain yield was used as the primary criterion with which to evaluate the optimal agricultural management practice. Regression analyses of either F_T or T with the LAI, crop yield and WUE were all performed to investigate the relationships between the partitioning of ET and crop development.

3 Results

3.1 Isotopic compositions of different waters

The LMWL was established as δD = 7.3 δ^{18}O + 3.6 (R^2 = 0.97, p < 0.01) and δD = 6.7 δ^{18}O + 1.8 (R^2 = 0.97, p < 0.01) for the 2014 and 2015 experimental seasons, respectively (Fig. 1). The smaller slope of the LMWL in 2015 than in 2014 was ascribed to a faster evaporation rate of falling raindrops (Wang et al., 2010b). As shown in Fig. 1, the soil water isotopes mainly fell below the LMWL, especially in 2015. The slope of the fitting line between δD and δ^{18}O in soil water was lower in 2015 (2.8) than in 2014 (4.0). It indicated that the soil water was more strongly evaporated in 2015.

According to two-way Analysis of variance (ANOVA), the isotopic profiles of the soil water showed significant differences among the different layers and growth stages (p < 0.05). The δD and δ^{18}O values of the soil water in the surface layer (0-20 cm) were remarkably enriched and indicated that the soil water isotopes had been subjected to extremely evaporative fractionation. The soil water isotope values in the 0-20 cm layer were significantly different from those in the other layers throughout the growing seasons (p < 0.05). The soil water isotopes in the 20-70 and 70-150 cm layers were intensively fractionated since the jointing stage. No significant seasonal changes were detected in the isotopic compositions of the soil water in the 150-200 cm layer, and they were similar to those values of irrigation water (Fig. 1). The stem water isotopes were mainly concentrated along the fitting line of the δD-δ^{18}O relationship in soil water (Fig. 1). The majority of the stem water isotopes in 2014 matched well with the soil water isotopes in the 0-150 cm layer; nevertheless, they were more enriched in 2015 and fell in the upper soil layer (0-70 cm). Therefore, the maximum root water uptake depth of winter wheat probably approached 150 cm during the experimental seasons.

3.2 Seasonal changes in soil water storage and ET

Approximately 127.9 mm of the soil water storage in the profile of 0-200 cm was consumed on average throughout the whole season from wheat greening to harvest. Approximately 92% of this consumption occurred in the 0-150 cm layer (Fig. 2). The slight change in the soil moisture within the 150-200 cm layer was consistent with the small variation in the soil water isotopic compositions in the same layer (Figs. 1-2). A greater amount of soil water storage (with a mean value of 35.2 mm) was consumed in 2015 than in 2014, primarily within the 0-70 cm layer (Fig. 2). The largest reduction in the soil water storage during the 2015 season occurred during the jointing-heading period (98.1 mm), and this reduction accounted for 67.4% of the total loss. Among the five treatments, T4 showed the highest consumption of soil water storage during the 2014 (151.8 mm) and 2015 (174.5 mm) seasons. Sufficient irrigation during treatment T5 in 2014 led to the smallest observed reduction in the soil water storage (80.3 mm). However, the reduction in the soil water storage under treatment T5 notably increased to 143.4 mm in 2015. This was primarily caused by severe reductions in the soil water storage during the jointing-heading and filling-harvest periods without irrigation under dry climatic conditions.

The total ET throughout the season from wheat greening to harvest was a mean of 292.8 mm with a standard deviation (SD) of 38.2 mm (Table 4). The total ET increased on average by 45.3 mm in 2015 relative to 2014, and this was in general agreement with the observed increment of soil water consumption in 2015. The reference agricultural management practice (T5) remarkably raised the crop water consumption in terms of the largest ET value in the growing seasons of both 2014 (304.0 mm) and 2015 (377.3 mm). The daily mean ET was significantly different (p < 0.01) among the four growth periods with values of 3.0, 5.0, 5.4, and 4.0 mm d^{-1} in the greening-jointing, jointing-heading, heading-filling, and filling-harvest periods, respectively. The higher daily mean ET flux during the mid-season stage (i.e., the jointing-filling stage) was mainly due to a higher LAI and an increased biomass.

3.3 Seasonal variations in ET partitioning

The seasonal variations in the partitioning of ET are shown in Fig. 3. The daily mean T changed significantly among the different periods during the experimental seasons of both 2014 and 2015 (p < 0.01) (Fig. 3). The daily mean T was evidently small (2.0 mm d^{-1}) during the early growth stage of greening-jointing and reached a high level during the jointing-heading and heading-filling periods (4.4 and 4.6 mm d^{-1}, respectively), after which it declined moderately to 3.4 mm d^{-1} until the winter wheat harvest. In contrast to T, a substantial seasonal variance in the daily mean E was detected only in 2014 with values of 1.1, 0.3, 0.8, and 0.6 mm d^{-1} during the greening-jointing, jointing-heading, heading-filling, and filling-harvest periods, respectively (Fig. 3). In 2015, the differences in the daily mean E among the four periods were small with an average value of 0.8 mm d^{-1}. A significant difference in the daily mean E between 2014 and 2015 occurred in the jointing-heading period, as it increased to 1.0 mm d^{-1} in 2015 due to severe drought induced by little precipitation and the lack of irrigation.

The values of F_T varied widely from 0.51 to 0.98 during the individual growth periods under different treatments. The mean values of F_T were 0.65, 0.88, 0.84, and 0.85 during the greening-jointing, jointing-heading, heading-filling, and filling-harvest periods, respectively

(Fig. 4). These results demonstrate that the average F_T during the jointing-heading period of the 2015 season (0.82) was much lower than that of the 2014 season (0.94). In particular, the decreasing of F_T in the jointing-heading period from 2014 to 2015 was evident under treatments T1, T2, and T5 with reductions of 0.25, 0.14 and 0.16, respectively. Moreover, the performance of F_T in each growth period was notably distinct among the different treatments (Fig. 4). Compared with the mean level of F_T for all of the treatments, F_T was 16.9% larger during the greening-jointing period but significantly less (17.6%, $p < 0.05$) during the filling-harvest period under treatment T1. The T5 under the reference agricultural management practices had the smallest F_T during greening-jointing period in 2015.

The F_T value during the whole season had an average value of 0.82, and it did not vary significantly among the seasons and treatments (with an SD of 0.03, $p > 0.05$) (Table 4). The T during the jointing-heading and heading-filling periods (T_{jf}) accounted for approximately 50% of the seasonal ET, and T_{jf} exhibited a significant positive linear correlation with the total ET ($R^2 = 0.82$, $p < 0.01$). Therefore, T_{jf} played a critical role in determining the variations in ET throughout the growing season. Fig. 4 demonstrates that the value of T_{jf} was greatly different between the two experimental seasons. The average T_{jf} was 34.9 mm more in 2015 than in 2014, occupying 76.9% of the increment (45.3 mm) in the total ET from 2014 to 2015. Furthermore, both the largest T_{jf} and the highest total ET were observed under the reference treatment (T5) in 2015.

Fig. 5 reveals that F_T increased with the LAI and varied around an asymptotic value of 0.87 when the LAI was between 2.7 and 8.7. The value of F_T was low with an average of 0.64 during the early growth stage (i.e., the greening-jointing period) with small LAI values

(0.7-2.0), while T was the predominant partition in the ET during the mid-growing season when the LAI exceeded 2.7 (Fig. 5). However, F_T reached a maximum of 0.78 with a small LAI (1.11) under treatment T1 during the 2015 season. The seasonal changes in F_T can be effectively described as a power-law function of the LAI (F_T = 0.61 LAI $^{0.21}$, R^2 = 0.66, p<0.01) for winter wheat (Fig. 5). This implied that crop development played a major role in driving the contribution of T to ET and that the LAI could provide insights into estimating the variability in F_T throughout the growing season of winter wheat.

3.4 Seasonal variations in root water uptake patterns

The contributions from soil water in different layers to root water uptake estimated using the MixSIAR model are shown in Fig. 6. The average contributions of soil water to winter wheat within the 0-20, 20-70, 70-150, and 150-200 cm layers during the 2014 growing season were 28.7%, 30.0%, 26.9%, and 14.4%, respectively. The root water uptake depth tended to become deeper with crop development (Fig. 6a). Winter wheat mainly acquired soil water from the 0-20 cm (63.6%), 20-70 cm (67.9%), 70-150 cm (54.4%), and 70-150 cm (39.8%) layers during the greening-jointing, jointing-heading, heading-filling, and filling-harvest growth periods, respectively. The 150-200 cm layer contributed a certain amount of soil water to winter wheat since the jointing-heading period and reached a maximum mean proportion of 27.2% in the filling-harvest period.

As shown in Fig. 6, higher quantities of shallow soil water were taken up by winter wheat in 2015, particularly within the top layer (0-20 cm) with average contributions of 28.7% and 42.6% in 2014 and 2015, respectively. The predominant water uptake depth was 0-20 cm in both the greening-jointing period (70.4%) and the heading-filling period (63.4%) in 2015.

During the jointing-heading period, the limited water supply and high T rates remarkably promoted the average contribution of deep soil water with values of 32.2% and 23.5% in the 70-150 cm and 150-200 cm layers, respectively. Meanwhile, winter wheat took up significantly more soil water from the 20-70 cm layer (54.9%) during the filling-harvest period than during the other periods ($p < 0.01$).

3.5 Relationships between grain yield and WUE with seasonal partition of ET

The crop yield and WUE of winter wheat throughout the growing season for each treatment are shown in Table 4. The mean grain yield was 6759.9 kg ha^{-1} with an SD of 478.5 kg ha^{-1}. Compared with the reference treatment, the T1, T2, and T3 treatments reduced the grain yield by more than 10%, while treatment T4 raised the yield by 0.9% for the 2014 season. Treatment T5 exhibited the lowest grain yield in the 2015 season, while the other treatments showed a 15.6% increment on average. The mean WUE was 24.9 kg ha^{-1} mm^{-1} in the 2014 season and 21.9 kg ha^{-1} mm^{-1} in the 2015 season. The variability in the WUE among the different treatments was greater in 2015 than in 2014. The maximum WUE was observed under T1, whereas T5 showed the smallest WUE in each season.

The results demonstrate that both the grain yield and the WUE were not significantly correlated with the F_T throughout the experimental season ($p > 0.05$). The observed grain yield positively increased with T_{jf} in 2014, whereas it decreased with T_{jf} in 2015. The grain yield reduced remarkably with excessive values of T_{jf} (205.8 mm) under treatment T5 in 2015 (Fig. 7 and Table 4). A significant quadratic relationship was found between the grain yield and T_{jf} ($R^2 = 0.77$, $p < 0.01$) (Fig. 7). The peak grain yield was 7062.6 kg ha^{-1} at a T_{jf} value of 155.8 mm along this fitting curve. The WUE also had a significant quadratic correlation with T_{jf} ($R^2 = 0.87$, $p < 0.01$) (Fig. 7). The peak WUE along the fitting curve was 24.9 kg ha^{-1} mm^{-1} with a T_{jf} value of 117.5 mm. Most T_{jf} values were larger than this critical value except for that under treatment T3 in 2014. As T_{jf} exceeded 117.5 mm, the WUE declined to a minimum value of 16.0 kg ha^{-1} mm^{-1} with a continuous increase in T_{jf} (Fig. 7). This suggested that the magnitude of T_{jf} controlled both the grain yield and the WUE for winter wheat in this region.

4 Discussion

4.1 Influencing factors of seasonal variations in ET partitioning

The daily T flux estimated in this study (ranging from 2.0 to 4.6 mm d^{-1}) was similar to those of 1.02-4.91 mm d^{-1} (Zhang et al., 2011) and 0.8-4.5 mm d^{-1} (Liu et al. 2002) under surface irrigation in the NCP determined via the isotope/eddy covariance and weighing/micro-lysimeters methods, respectively. E is a significant component of ET, especially when the LAI is low. The seasonal F_E (0.18) was also in accordance with the value of 0.23 reported by Liu et al. (2002). The F_E value calculated in our study reached up to 0.35 during the greening-jointing period, which is consistent with the estimation of 0.30 from Zhang et al. (2011). This study indicated that the seasonal changes in F_T could be effectively described through a power-law function of the LAI. This relationship was similar to those obtained in recent studies at both the global and the field scale (Wang et al., 2014; Wei et al., 2015; Wu et al., 2017; Lu et al., 2017). The strong correlation between F_T and LAI confirmed that F_T was controlled by LAI at seasonal timescale (Wang and Yamanaka, 2014; Wang et al., 2014; Wei et al., 2015; Wei et al., 2018). When LAI was less than 2.7, F_T increaseed significantly with crop development in the early growing season and then it converged towards a stable value beyond LAI of 2.7. This threshold of LAI (2.7) to distinguish the two different changing trends of F_T agreed well with the values of 2.5 and 3.0 reported in Wei et al. (2018) and Kang et al. (2003), respectively. F_T has been shown to reach a high level (0.90 for agricultural systems at the global scale and 0.58 for a paddy field), even under low LAI conditions (Wang et al., 2014; Wei et al., 2015). In this study, the estimated F_T reached up to 0.78 with a small LAI (1.11) under treatment T1 during the 2015 growing season. The above comparisons indicate that the ET partitioning results in this study are reliable.

Besides LAI, F_T was influenced greatly by soil moisture, especially the topsoil moisture in 0-20 cm depth. Previous studies indicated that F_T generally decreased with increasing topsoil moisture due to increase of E under the same LAI conditions (Liu et al., 2002; Yu et al., 2009; Wei et al., 2018). A negative linear correlation was found between F_T and surface soil water content (θ_v) when LAI was about 1.8 (F_T=-1.38θ_v+1.0, R^2=0.98, p<0.01) during greening-jointing period in our experiments. It was suggested that keeping surface soil dry without affecting the crop ET was an important way to reduce E in the early growing season (Liu et al., 2002). However, increasing θ_v remarkably increased F_T at LAI of about 4.0 (F_T=1.83θ_v+0.6, R^2=0.74, p<0.01) during filling-harvest period.

Factors controlling E and T were coupled in ways to affect F_T under dry climate condition particularly during jointing-heading period in 2015. Adequate rainfall falling during greening-jointing period (35 mm) led to larger θ_v at the early stage in jointing-heading period (mean of 0.19). Great availability of soil moisture in the topsoil increased water contribution to E. Furthermore, the strong atmosphere demand remarkably promoted E at late stage of the jointing-heading period (Zhao et al., 2018). This resulted in the significant increase of the E rate to 1.0 mm d^{-1} in the period. It was the topsoil moisture greatly influencing E, while the water used for T came from the whole root zone. Although continuous E caused the extreme consumption of surface soil moisture in the drought period, soil water storage in the subsurface layers could meet T requirement of crop. Soil water in the deep layers could move into the upper dry layer via hydraulic lift through the process of root water uptake (Jha et al, 2017; Li et al., 2010). High water uptake from deep layers (32.2% and 23.5% in the 70-150 cm and 150-200 cm layers, respectively) may improve the plant leaf water content and maintain T rates and dry matter production.

Distributions of soil moisture and root water uptake patterns were significantly influenced by different irrigation and fertilization treatments especially in dry seasons. More frequently irrigated treatments have previously been reported to have more roots in the surface layer than less irrigated treatments (Zhang et al., 2004). Meanwhile, nitrogen fertilizers stimulated root growth near the soil surface and abundant soil nitrogen content might increase the drought resistance of the root system under water limited condition (Kmoch et al., 1957; Carvalho and Foulkes, 2013). Ma and Song (2016) showed that the soil water contribution had a significantly positive and linear relationship with the proportion of root length. Therefore, plant primarily took up soil water from the top layer (0-20 cm) under the T4 and T5 treatments even though the climate was dry during jointing-heading period in 2015. However, nitrogen deficiency promoted root growth in the deep soil layer (150-200 cm) and increased water adsorption by 43.1% under the T1 and T3 treatments. Previous studies demonstrated that plants growing in drier environments with soil water deficit in the surface layer have deeper root systems and more branched seminal roots (Morita et al., 1997; Zhang et al., 2004; Jha et al., 2017). This confirmed that over 80% of plant water took up soil water from the 70-200 cm layer under the less irrigation treatments of T1 and T2. When soil water near the surface was replenished by irrigation, the extraction depth returned to the surface layer (such as in heading-filling period) and subsequently moved downward again until harvest of winter wheat.

4.2 Application for optimizing water management practices

With the abovementioned ET partitioning results and the fitted WUE-T_{jf} and Yield-T_{jf} curves, the irrigation and fertilization schedules were optimized. As shown in Fig. 7, the value of T_{jf} should be controlled between 117.5 and 155.8 mm to obtain both a high grain yield and a high WUE. The T_{jf} under treatments T1, T2, T4, and T5 in 2014 and that under treatment T1 in 2015 acquired in this study were within this range. An additional irrigation of 140 mm was required for treatment T5 compared with the T1. Although the T1 treatment in 2014 had a larger WUE, its grain yield was diminished by 8.5% relative to 2015. Therefore, the T1 treatment in 2015 optimally improved the WUE and maintained a high grain yield. The optimal irrigation and fertilization schedules can be determined as two irrigations during the greening-jointing (20 mm) and heading-filling (80 mm) periods and one fertilization (105 kg ha^{-1} N) during the greening-jointing period. The designed wetting layer should be controlled at depths of 0-70 cm because wheat primarily sourced soil water from the 0-70 cm layer during the experimental seasons. This practice could make better use of the deep soil water storage and avoid deep percolation compared with a traditional wetting depth of 100 cm (Zhang et al., 2011).

The obtained optimal agricultural management practice is supported by previous studies in the NCP. The first small irrigation was applied mainly to the top soil to ensure that the fertilization was distributed evenly throughout the plot. The irrigation in the early growth stage reduced the grain yield because it enhanced the development of non-functional tillers, which consume the reserved nutrients (Sun et al., 2006). Wang et al. (2014) and Lu et al. (2017) reported that water loss via E could be much higher during the vegetative stage than during later growth stages. Reducing the irrigation amount during the greening-jointing period could increase the depletion of deep soil water, and it was definitely necessary to improve the WUE of winter wheat. Meanwhile, the heading growth period was extremely sensitive to water stresses, and irrigation is strongly recommended during this period (Zhang et al., 2003; Li et al., 2005; Shang and Mao, 2006). Therefore, the obtained optimal schedule in this study is appropriate, as it could conserve 140 mm of irrigation water and 105 kg ha^{-1} N of fertilizer with respect to the reference practices.

4.3 Further scopes of this study

The ET of winter wheat was partitioned effectively into E and T using the isotope mass balance and water balance methods. The partitioning of ET changed between different irrigation and fertilization schedules and various crop development stages. The evaluation using isotopic data presented a quantitative correlation between seasonal change in the F_T and the crop development of LAI. The relationships among the grain yield and WUE with the T_{jf} were discovered. This isotope-based method provided insights into clarifying the hydrological processes in field ecosystem and optimizing water and nitrogen management practices. Nevertheless, several issues still need further investigation. First, although the interception flux is often neglected in many partitioning works, it indeed is a component of

ET besides E and T and need further estimation. Second, the water flux at the bottom boundary of the soil profile was generally neglected in the estimation of ET due to small changes in soil moisture during winter wheat growing season under limited irrigation in the NCP (Zhang et al., 2003; Li et al., 2005; Li et al., 2010). However, drainage should be accurately evaluated by the Darcy's law when soil moisture at the bottom boundary is above field capacity. Third, as calculated from the MixSIAR model, each soil layer had a different contribution to the root water uptake. Incorporating these contributions into the isotopic mass balance equation can reflect the variation in the gradient of the isotopic profile. Finally, high-frequency measurements of isotopic composition of soil, stem and gas water will improve understanding the seasonal variation in ET partitioning.

4 Conclusions

In this study, the isotope mass balance were coupled with water balance methods for the partitioning of evapotranspiration (ET) into crop transpiration (T) and soil evaporation (E) of winter wheat under different irrigation and fertilization treatment schemes during 2014-2015 in Beijing, China. The fraction of T in ET (F_T) showed averages of 65.4%, 87.7%, 83.8%, and 84.9% in the greening-jointing, jointing-heading, heading-filling, and filling-harvest periods, respectively. The performance of F_T was notably distinct among the different treatments in each growing period. However, the value of F_T throughout the season from greening to harvest did not vary significantly among the seasons and treatments (p > 0. 05) and had an average value of 0.82. The seasonal change in F_T could be effectively described as a power-law function of the LAI ($F_T = 0.61\ \mathrm{LAI}^{0.21}$, $R^2 = 0.66$, $p<0.01$). Winter wheat mainly utilized soil water from the 0-20 cm (67.0%), 20-70 cm (42.0%), 0-20 cm (38.7%), and 20-70

Hydrol. Earth Syst. Sci. Discuss., https://doi.org/10.5194/hess-2018-234
Manuscript under review for journal Hydrol. Earth Syst. Sci.
Discussion started: 14 May 2018

cm (34.9%) layers during the greening-jointing, jointing-heading, heading-filling, and filling-harvest periods, respectively. The main root water uptake depth increased with the crop development in 2014, whereas it was mostly concentrated within the 0-70 cm layer in 2015. F_T was not significantly correlated with the grain yield and WUE ($p > 0.05$), and the total T during the jointing-heading and heading-filling periods (T_{jf}) had a significant quadratic relationship with the grain yield and WUE ($p < 0.01$). In order to obtain the optimal crop yield, 20 mm and 80 mm of irrigation water during the greening-jointing and heading-filling periods, and 105 kg ha^{-1} N of fertilization during the greening-jointing period were needed. The designed wetting layer should be controlled at depths of 0-70 cm. This study demonstrated the roles of seasonal ET partitioning obtained via isotope-based methods in determining the crop development and improving the WUE, and the findings acquired herein have important implications on irrigation and fertilization management.

Acknowledgements. This work was supported by the National Natural Science Foundation of China (Grant No. 41671027; 41730749). We thank Ningxia Sun for field data collection and Dr. Baozhong Zhang and Lihu Yang for their assistance in field and laboratory experiments.

References

Agam, N., Evett, S.R., Tolk, J.A., Kustas, W.P., Colaizzi, P.D., Alfieri, J.G., McKee, L.G., Copeland, K.S., Howell, T.A., and Chávez, J.L.: Evaporative loss from irrigated interrows in a highly advective semi-arid agricultural area, Adv. Water Res., 50, 20-30, 2012.

Hydrol. Earth Syst. Sci. Discuss., https://doi.org/10.5194/hess-2018-234
Manuscript under review for journal Hydrol. Earth Syst. Sci.
Discussion started: 14 May 2018

Allison, G.B. and Barnes, C.J.: Estimation of evaporation from non-vegetated surfaces using natural deuterium, Nature, 301, 143-145, 1983.

Aouade, G., Ezzahar, J., Amenzou, N., Er-Raki, S., Benkaddour, A., Khabba, S., and Jarlan, L.: Combining stable isotopes, Eddy Covariance system and meteorological measurements for partitioning evapotranspiration, of winter wheat, into soil evaporation and plant transpiration in a semi-arid region, Agric. Water Manag., 177, 181-192, 2016.

Asbjornsen, H., Mora, G., and Helmers, M.J.: Variation in water uptake dynamics among contrasting agricultural and native plant communities in the Midwestern US, Agric. Ecosyst. Environ., 121, 343-356, 2007.

Ben-Gal, A.and Shani, U.: Yield, transpiration and growth of tomatoes under combined excess boron and salinity stress. Plant Soil. 247, 211-221, 2002.

Brunel, J.P., Walker, G.R., Dighton, J.C., and Monteny, B.: Use of stable isotopes of water to determine the origin of water used by the vegetation and to partition evapotranspiration. A case study from HAPEX-Sahel, J. Hydrol., 188-189, 466-481, 1997.

Burt, C.M., Mutziger, A.J., Allen, R.G., and Howell, T.A.: Evaporation research: Review and interpretation, J. Irrigation Drainage Eng., 131, 37-58, 2005.

Cai, J.B., Liu, Y., Xu, D., Paredes, P., and Pereira, L.S.: Simulation of the soil water balance of wheat using daily weather forecast messages to estimate the reference evapotranspiration, Hydrol. Earth Syst. Sci., 13, 1045-1059, 2009.

Carvalho, P. and Foulkes, M.J.: Roots and uptake of water and nutrients. In: Christou, P., Savin, R., Costa-Pierce, B., Misztal, I., Whitelaw, C.B. (Eds.), Sustainable Food Production. Springer, NewYork, pp. 1390-1404, 2013.

Hydrol. Earth Syst. Sci. Discuss., https://doi.org/10.5194/hess-2018-234
Manuscript under review for journal Hydrol. Earth Syst. Sci.
Discussion started: 14 May 2018

Hydrology and Earth System Sciences
Open Access
Discussions

Cavanaugh, M. L., Kurc, S. A., and Scott, R. L. Evapotranspiration partitioning in semiarid shrubland ecosystems: A two-site evaluation of soil moisture control on transpiration, Ecohydrology, 4, 671-681, 2011.

Clark, I.D. and Fritz, P. Environmental Isotopes in Hydrogeology, Lewis Publishers, New York, 1997.

Coenders-Gerrits, A. M. J., van der Ent, R. J., Bogaard, T. A., Wang-Erlandsson, L., Hrachowitz, M., and Savenije, H. H. G.: Uncertainties in transpiration estimates, Nature, 506, E1-E2, doi:10.1038/nature12925, 2014.

Ding, R.S., Kang, S.Z., Zhang, Y.Q., Hao, X.M., Tong, L., and Du, T.S. Partitioning evapotranspiration into soil evaporation and transpiration using a modified dual crop coefficient model in irrigated maize field with ground-mulching, Agric. Water Manag., 127, 85-96., 2017.

Guan, H.D. and Wilson, J.L.: A hybrid dual-source model for potential evaporation and transpiration partitioning, J. Hydrol., 377, 405-416, 2009.

Hanks, R.J., Jame, D.W., and Watts, D.W.: Irrigation management and crop production as related to nitrate mobility. p. 141-151. In Chemical mobility and reactivity in soil systems. ASA and SSSA, Madison, WI., 1983.

Hsieh, J.C.C., Chadwick, O.A., Kelly, E.F.,and Savin, S.M.: Oxygen isotopic composition of soil water: quantifying evaporation and transpiration, Geoderma, 82, 269-293, 1998.

Hussain, G., Al-Jaloud, A.A., Al-Shammary, S.F., and Karimulla, S. Effect of saline irrigation on the biomass yield and the protein, nitrogen, phosphorus and potassium composition of alfalfa in a pot experiment, J. Plant Nutr., 18, 2389-2408, 1995.

Jha, S.K, Gao, Y., Liu, H., Huang, Z.D., Wang, G.S., Liang, Y.P., and Duan, A.W.: Root development and water uptake in winter wheat under different irrigation methods and scheduling for North China, Agric. Water Manage., 182, 139-150, 2017.

Kang, S.Z., Gu, B.J., Du, T. S., and Zhang, J. H.: Crop coefficient and ratio of transpiration to evapotranspiration of winter wheat and maize in a semi-humid region, Agric. Water Manag., 59, 239-254, 2003.

Kato, T., Kimura, R., Kamichika, M.: Estimation of evapotranspiration, transpiration ratio and water-use efficiency from a sparse canopy using a compartment model, Agric. Water Manag., 65, 173-191, 2004.

Kmoch, H. G., Ramig, R. E., Fox, R. L., and Koehler, F. E.: Root development of winter wheat as influenced by soil moisture and nitrogen fertilization, Agron. J., 49, 20-26, 1957.

Kool, D., Agam, N., Lazarovitch, N., Heitman, J. L., Sauer, T. J., and Ben-Gal, A.: A review of approaches for evapotranspiration partitioning, Agric. For. Meteor., 184, 56-70, 2014.

Kustas, W.P. and Agam, N.: Soil evaporation. In: Wang, Y.Q. (Ed.), Encyclopedia of Natural Resources, Taylor & Francis, New York, 2013.

Li, J.M., Inanaga, S., Li, Z.H., and Eneji, A.E.: Optimizing irrigation scheduling for winter wheat in the North China Plain, Agric. Water Manage., 76, 8-23, 2005.

Li, Q.Q., Dong, B.D., Qiao, Y.Z., Liu, M.Y., and Zhang, J.W.: Root growth, available soil water, and water-use efficiency of winter wheat under different irrigation regimes applied at different growth stages in North China, Agric. Water Manage., 97, 1676-1682, 2010.

Liu, C.M., Zhang, X.Y., and Zhang, Y.Q.: Determination of daily evaporation and evapotranspiration of winter wheat and maize by large-scale weighing lysimeter and micro-lysimeter, Agr. For. Meteorol., 111, 109-120, 2002.

Liu, X.W., Shao, L.W., Sun, H.Y., Chen, S.Y., and Zhang, X.Y. Responses of yield and water use efficiency to irrigation amount decided by pan evaporation for winter wheat, Agric. Water Manag., 129, 173-180, 2013.

Lu, X.F., Liang, L.L., Wang, L.X., Jenerette, G.D., McCabe, M.F., and Grantz, D.A. Partitioning of evapotranspiration using a stable isotope technique in an arid and high temperature agricultural production system, Agr. Water Manage., 179, 103-109, 2017.

Ma, Y. and Song, X.F.: Using stable isotopes to determine seasonal variations in water uptake of summer maize under different fertilization treatments, Sci. Total Environ., 550, 471-483, 2016.

McCole, A.A. and Stern, L.A.: Seasonal water use patterns of Juniperus ashei on the Edwards plateau, Texas, based on stable isotopes in water, J. Hydrol., 342, 238-248, 2007.

Mitchell, P. J., Veneklaas, E., Lambers, H., and Burgess, S. S. O.: Partitioning of evapotranspiration in a semi-arid eucalypt woodland in south-western Australia, Agr. Forest Meteorol., 149, 25-37, 2009.

Moore, J.W. and Semmens, B.X.: Incorporating uncertainty and prior information into stable isotope mixing models, Ecol. Lett., 11, 1-11, 2008.

Morita, S., Okuda, H., and Abe, J.: Root system morphology of wheat grown under different soil moisture and transpiration rates after rehydration, J. Agric. Meteorol., 52, 819-822, 1997.

Hydrol. Earth Syst. Sci. Discuss., https://doi.org/10.5194/hess-2018-234
Manuscript under review for journal Hydrol. Earth Syst. Sci.
Discussion started: 14 May 2018

Hydrology and Earth System Sciences
Open Access
Discussions

Newman, B.D., Wilcox, B.P., Archer, S.R., Breshears, D.D., Dahm, C.N., Duffy, C.J., McDowell, N.G., Phillips, F.M., and Scanlon, B.R.: Ecohydrology of water-limited environments: A scientific vision, Water Res. Res., 42, 10.1029/2005WR004141, 2006.

Phillips, D.L. and Gregg, J.W.: Source partitioning using stable isotopes: coping with too many sources, Oecologia, 136, 261-269, 2003.

Robertson, J.A. and Gazis, C.A.: An oxygen isotope study of seasonal trends in soil water fluxes at two sites along a climate gradient in Washington State (USA), J. Hydrol., 328, 375-387, 2006.

Shang, S.H. and Mao, X.M.: Application of a simulation based optimization model for winter wheat irrigation scheduling in North China, Agric. Water Manage., 85, 314-322, 2006.

Sprenger, M., Leistert, H., Gimbel, K., and Weiler, M.: Illuminating hydrological processes at the soil-vegetation-atmosphere interface with water stable isotopes, Rev. Geophys., 54, doi:10.1002/2015RG000515, 2016.

Stanhill, G.: Evaporation, transpiration and evapotranspiration: A case for Ockham's Razor. In: Hadas A, Swartzendruber D, Rijtema PE, Fuchs M, Yardn B, editors, Physical aspects of soil water and salts in ecosystems, Berlin: Verlag, p. 207-220, 1973.

Stock, B.C. and Semmens, B.X.: MixSIAR GUI User Manual, version 1.0. http://conserver.iugo-cafe.org/user/brice.semmens/MixSIAR, 2013.

Sun, H.Y., Liu, C.M., Zhang, X.Y., Shen, Y.J., and Zhang, Y.Q.: Effects of irrigation on water balance, yield and WUE of winter wheat in the North China Plain, Agr. Water. Manage., 85, 211-218, 2006.

Sutanto, S. J., Wenninger, J., Coenders-Gerrits, A. M. J., Uhlenbrook, S.: Partitioning of evaporation into transpiration, soil evaporation and interception: a comparison between isotope measurements and a HYDRUS-1D model, Hydrol. Earth Syst. Sci., 16, 2605-2616, 2012.

Sutanto, S., van den Hurk, B., Dirmeyer, P. A., Seneviratne, S. I., Röckmann, T, Trenberth K. E., Blyth, E. M., Wenninger, and J., Hoffmann, G.: A perspective on isotope versus non-isotope approaches to determine the contribution of transpiration to total evaporation., Hydrol. Earth Syst. Sci., 18, 2815-2827, 2014.

Tolk, J.A., Howell, T.A., Steiner, J.L., Krieg, D.R., and Schneider, A.D.: Role of transpiration suppression by evaporation of intercepted water in improving irrigation efficiency, Irrig. Sci., 16, 89-95, 1995.

Tolk, J.A. and Howell, T.A.: Transpiration and yield relationships of grain sorghum grown in a field environment, Agron. J., 101, 657-662, 2009.

Van Halsema, G.E., and Vincent, L.: Efficiency and productivity terms for water management: a matter of contextual relativism versus general absolutism, Agric.Water Manage., 108, 9-15, 2012.

Villalobos, F.J. and Ferres, E.: Evaporation measurements beneath corn, cotton and sun-flower canopies, Agon. J., 82, 1153-1159, 1990.

Wang, L.X., Caylor, K.K., Villegas, J.C., Barron-Gafford, G.A., Breshears, D.D., and Huxman, T.E.: Partitioning evapotranspiration across gradients of woody plant cover: Assessment of a stable isotope technique, Geophys. Res. Lett., 37, L09401, doi: 10.1029/2010GL043228, 2010a.

Hydrol. Earth Syst. Sci. Discuss., https://doi.org/10.5194/hess-2018-234
Manuscript under review for journal Hydrol. Earth Syst. Sci.
Discussion started: 14 May 2018

Wang, L.X., Good, S.P., and Caylor, K. K.: Global synthesis of vegetation control on evapotranspiration partitioning, Geophys. Res. Lett., 41, 6753–6757, 2014.

Wang, P., Song, X.F., Han, D.M., Zhang, Y.H., and Liu, X.: A study of root water uptake of crops indicated by hydrogen and oxygen stable isotopes: A case in Shanxi Province, China, Agric. Water Manag., 97, 475-482, 2010b.

Wang, P., Song, X.F., Han, D.M., Zhang, Y.H., and Zhang, B.: Determination of evaporation, transpiration and deep percolation of summer corn and winter wheat after irrigation, Agric. Water Manage., 105, 32-37, 2012.

Wang, P. and Yamanaka, T.: Application of a two- source model for partitioning evapotranspiration and assessing its controls in temperate grasslands in central Japan, Ecohydrology, 7, 345-353, 2014.

Wang, P., Li, X.Y., Huang, Y.M., Liu, S.M., Xu, Z.W., Wu, X.C., and Ma, Y.J.: Numerical modeling the isotopic composition of evapotranspirationin an arid artificial oasis cropland ecosystem with high-frequencywater vapor isotope measurement, Agric. For. Meteorol., 230-231, 79-88, 2016.

Wang, X. and Yakir, D.: Using stable isotopes of water in evapotranspiration studies, Hydrol. Process., 14, 1407-1421, 2000.

Wei, Z., W., Yoshimura, K., Okazaki, A., Kim, W., Liu, Z. F., and Yokoi, M.: Partitioning of evapotranspiration using high frequency water vapor isotopic measurement over a rice paddy, Water Resour. Res., 3716-3729, doi:10.1002/2014WR016737, 2015.

Hydrol. Earth Syst. Sci. Discuss., https://doi.org/10.5194/hess-2018-234
Manuscript under review for journal Hydrol. Earth Syst. Sci.
Discussion started: 14 May 2018

Wei, Z.W., Lee, X.H., Wen, X.F., and Xiao, W.: Evapotranspiration partitioning for three agro-ecosystems with contrasting moisture conditions: a comparison of an isotope method and a two-source model calculation, Agric. For. Meteor., 252, 296-310, 2018.

Wen, X.F., Yang, B., Sun, X.M., and Lee, X.H.: Evapotranspiration partitioning through in-situ oxygen isotope measurements in an oasis cropland, Agric. For. Meteor., 230-231, 89–96, 2016.

Wenninger, J., Beza, D.T., and Uhlenbrook, S.: Experimental investigations of water fluxes within the soil-vegetation-atmosphere system: Stable isotope mass-balance approach to partition evaporation and transpiration, Phys, Chem. Earth., 35, 565-570, 2010.

West, A.G., Patrickson, S.J., and Ehleringer, J.R.: Water extraction times for plant and soil materials used in stable isotope analysis, Rapid Commun. Mass Spectrom, 20, 1317-1321, 2006.

Wu, Y.J., Du, T.S., Ding, R. S., Tong, L., Li, S.E., and Wang, L. X.: Multiple methods to partition evapotranspiration in a maize field, J. Hydrometeor, 18, doi: 10.1175/JHM-D-16-0138.1, 2017.

Yang, B., Wen, X.F., and Sun, X.M.: Irrigation depth far exceeds water uptake depth in an oasis cropland in the middle reaches of Heihe, Sci. Rep., 5, 15206, doi: 10.1038/srep15206 (2015), 2015.

Yu, L.P., Huang, G.H., Liu, H.J., Wang, X.P., and Wang, M.Q.: Experimental investigation of soil evaporation and evapotranspiration of winter wheat under sprinkler irrigation, Agric. Sci. China, 8, 1360-1368, 2009.

Hydrol. Earth Syst. Sci. Discuss., https://doi.org/10.5194/hess-2018-234
Manuscript under review for journal Hydrol. Earth Syst. Sci.
Discussion started: 14 May 2018

Zhang, B.Z., Liu, Y., Xu, D., Zhao, N.N., Lei, B., Rosa, R.D., Paredes, P., Paço, T.A., and Pereira, L.S.: The dual crop coefficient approach to estimate and partitioning evapotranspiration of the winter wheat-summer maize crop sequence in North China Plain, Irrig. Sci., 31, 1303-1316, 2013.

Zhang, Y.C., Shen, Y.J., Sun, H.Y., and Gates, J.B. Evapotranspiration and its partitioning in an irrigated winter wheat field: A combined isotopic and micrometeorologic approach, J. Hydrol., 408, 203-211, 2011.

Zhang, X.Y., Pei, D., and Hu, C.S.: Conserving groundwater for irrigation in the North China Plain, Irrig. Sci., 21, 159-166, 2003.

Zhang, X.Y., Pei, D., and Chen, S.Y.: Root growth and soil water utilization of winter wheat in the North China Plain, Hydrol. Process., 18, 2275-2287, 2004.

Zhao, P., Kang, S.Z., Li, S.E., Ding, R.S., Tong, L., and Du, T.S.: Seasonal variations in vineyard ET partitioning and dual crop coefficients correlate with canopy development and surface soil moisture, Agric. Water Manage., 197, 19-33, 2018.

Zimmermann, U., Ehhalt, D., and Munnich, K.: Soil water movement and evapotranspiration: changes in the isotopic composition of the water. In: Proceedings of the IAEA Symposium on the Use of Isotopes in Hydrology, IAEA, Vienna, p. 567-584, 1967.

Hydrol. Earth Syst. Sci. Discuss., https://doi.org/10.5194/hess-2018-234
Manuscript under review for journal Hydrol. Earth Syst. Sci.
Discussion started: 14 May 2018

Hydrology and Earth System Sciences
Open Access
Discussions

Figure captions

Fig. 1. δD-δ^{18}O relationship for the water samples and the local meteoric water line (LMWL) in the (a) 2014 and (b) 2015 growing seasons.

Fig. 2. Seasonal variations in the soil moisture under the (a) T1, (b) T2, (c) T3, (d) T4, and (e) T5 treatments.

Fig. 3. Mean daily evaporation (E) and transpiration (T) rates of winter wheat during each growth period in the 2014 and 2015 seasons (mean ± SD). ○ and * represent outliers with a 1.5 × interquartile range (IQR) and a 3IQR, respectively.

Fig. 4. Seasonal variations in T, E, and the fraction of transpiration within evapotranspiration (F_T) in winter wheat for each treatment during (a) 2014 and (b) 2015.

Fig. 5. Relationship between the fraction of transpiration within evapotranspiration (F_T) and the leaf area index (LAI).

Fig. 6. Proportions of the soil water contribution to winter wheat during each growth stage in (a) 2014 and (b) 2015 (mean ± SD). ○ and * represent outliers with a 1.5× interquartile range (IQR) and a 3IQR, respectively.

Fig. 7. Relationships among the grain yield and water use efficiency (WUE) with the total transpiration during the jointing-heading and heading-filling periods (T_{jf}).

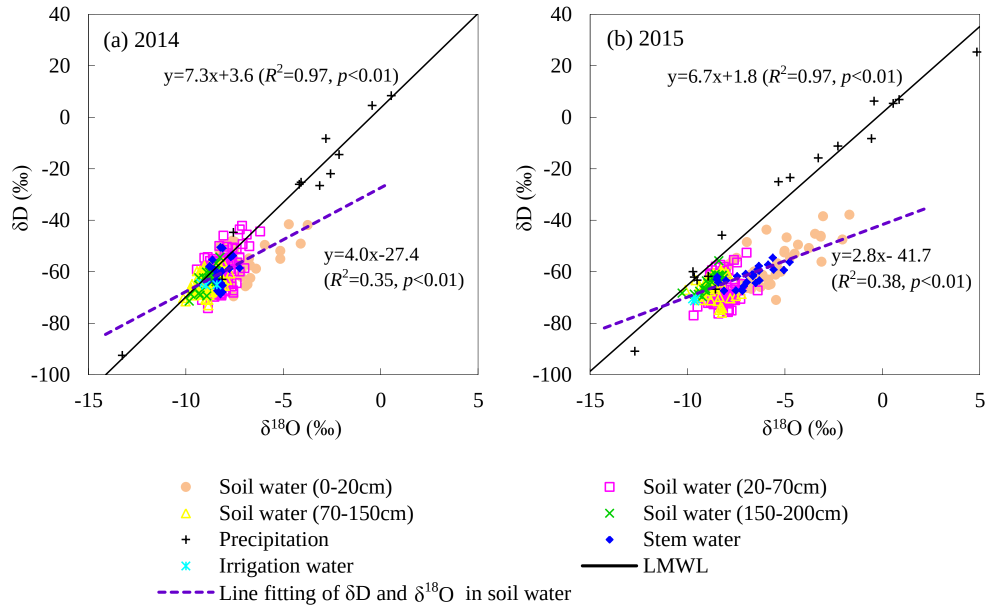

Fig.1. δD-δ^{18}O relationship for the water samples and the local meteoric water line (LMWL) in the (a) 2014 and (b) 2015 growing seasons.

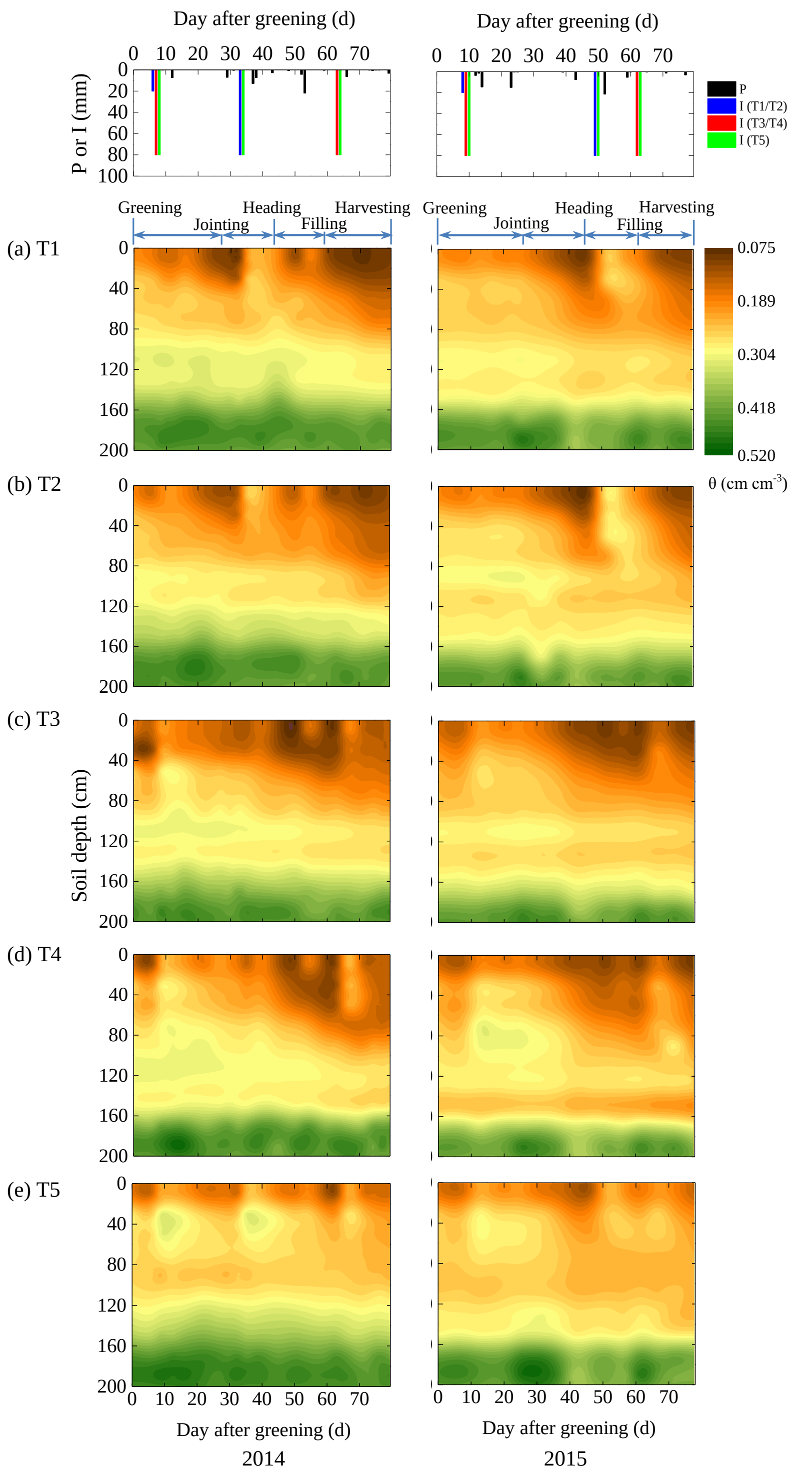

Fig.2. Seasonal variations in the soil moisture under the (a) T1, (b) T2, (c) T3, (d) T4, and (e) T5 treatments.

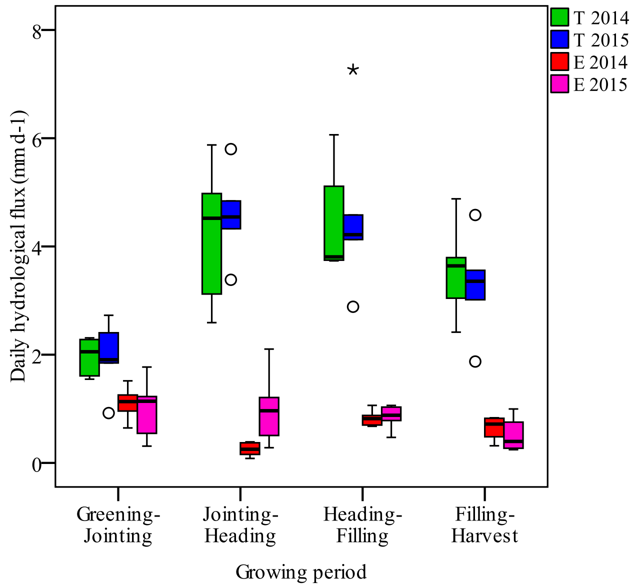

Fig.3. Mean daily evaporation (E) and transpiration (T) rates of winter wheat during each growth period in the 2014 and 2015 seasons (mean ± SD). ○ and * represent outliers with a 1.5× interquartile range (IQR) and a 3IQR, respectively.

Hydrol. Earth Syst. Sci. Discuss., https://doi.org/10.5194/hess-2018-234
Manuscript under review for journal Hydrol. Earth Syst. Sci.
Discussion started: 14 May 2018

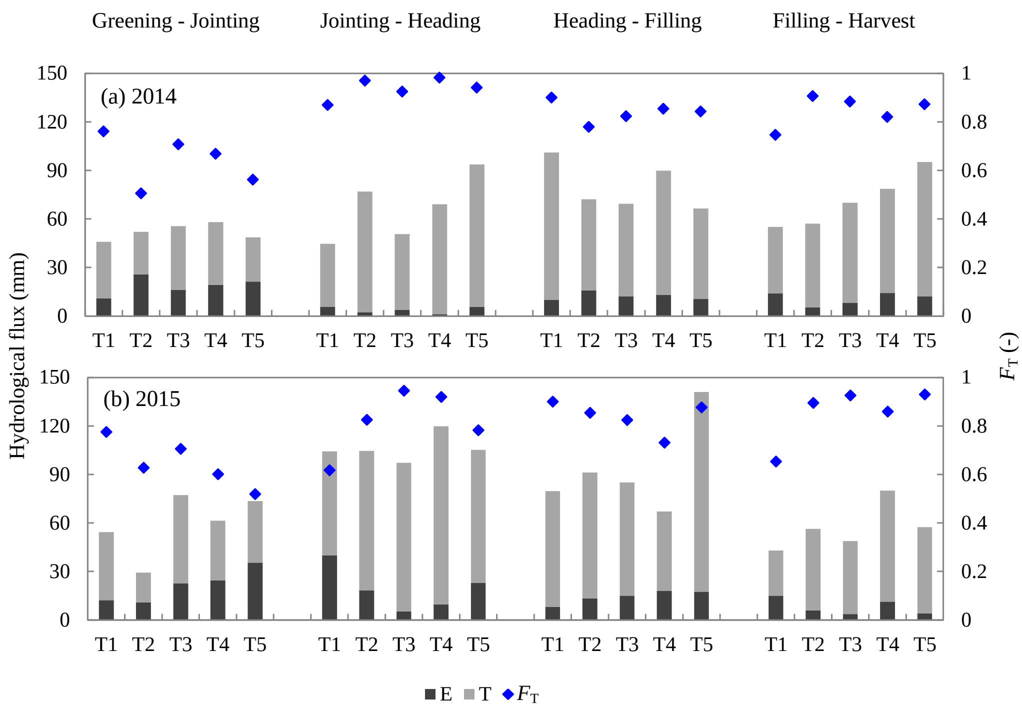

Fig.4. Seasonal variations in T, E, and the fraction of transpiration within evapotranspiration (F_T) in winter wheat for each treatment during (a) 2014 and (b) 2015.

Hydrol. Earth Syst. Sci. Discuss., https://doi.org/10.5194/hess-2018-234
Manuscript under review for journal Hydrol. Earth Syst. Sci.
Discussion started: 14 May 2018

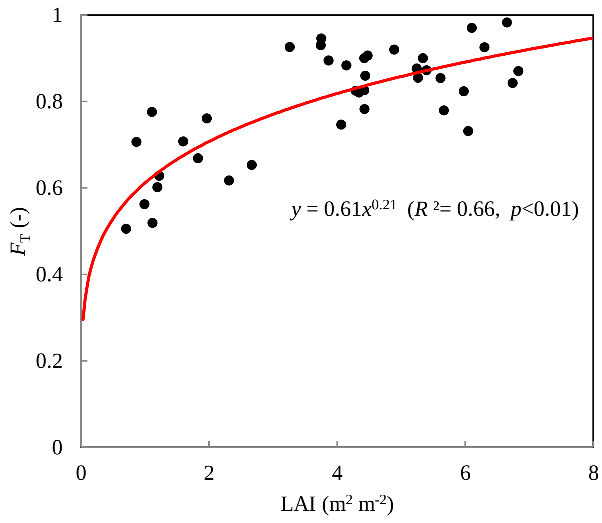

Fig.5. Relationship between the fraction of transpiration within evapotranspiration (F_T) and the leaf area index (LAI).

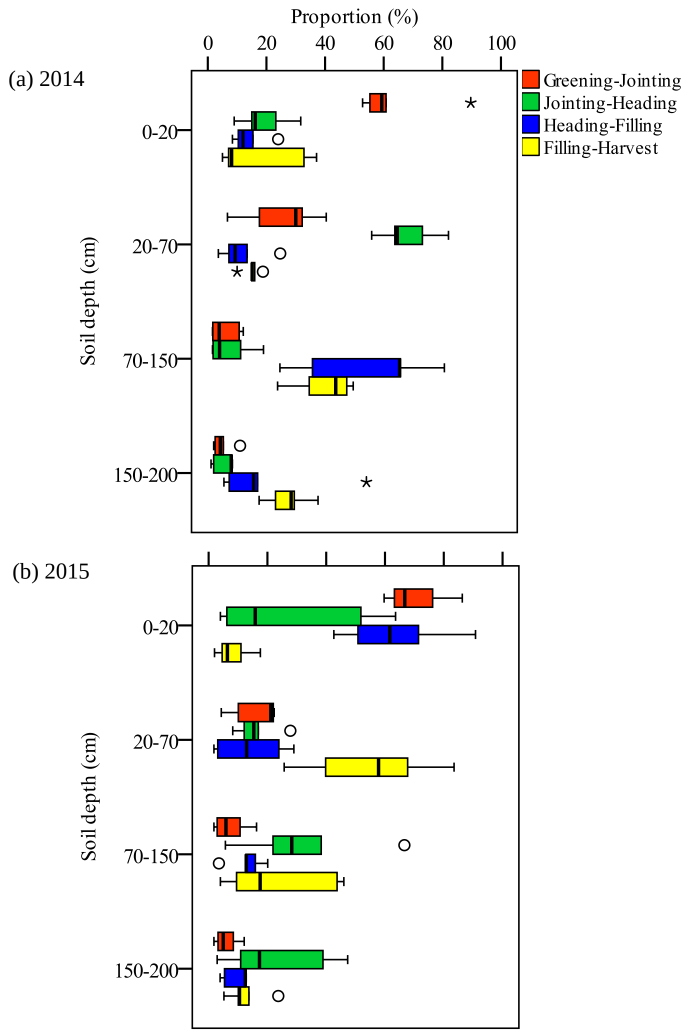

Fig.6. Proportions of the soil water contribution to winter wheat during each growth stage in (a) 2014 and (b) 2015 (mean ± SD). ○ and * represent outliers with a 1.5× interquartile range (IQR) and a 3IQR, respectively.

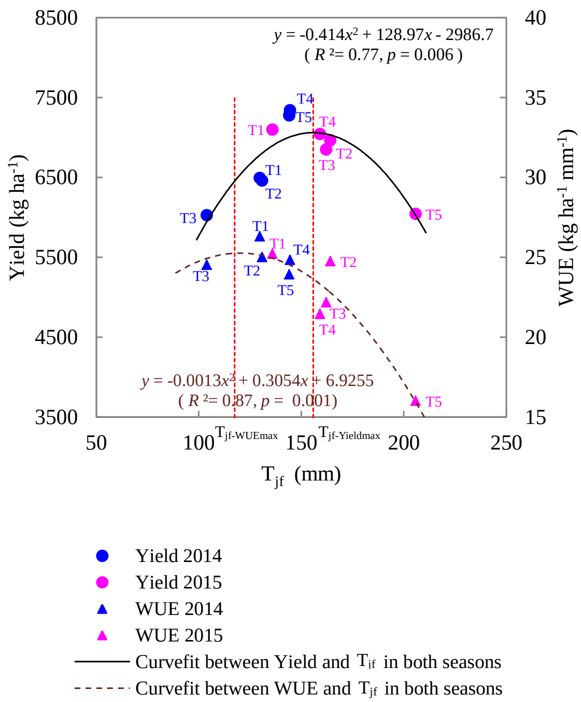

Fig.7. Relationships among the grain yield and water use efficiency (WUE) with the total transpiration during the jointing-heading and heading-filling periods (T_{jf}). The two vertical red dashed lines represented the T_{jf} under the maximum WUE ($T_{jf\text{-}WUEmax}$) and Yield ($T_{jf\text{-}Yieldmax}$) conditions.

Table 1. Physical and chemical properties of the soil profile at the experimental site.

Depth	Particle size (%)			Soil texture	Bulk density	θ_s	K_s	OC	EC	pH	NH_4^+-N	NO_3^--N
(cm)	Sand	Silt	Clay		(g cm^{-3})	(cm^3 cm^{-3})	(cm d^{-1})	(g kg^{-1})	(μS cm^{-1})		(mg kg^{-1})	(mg kg^{-1})
0-20	58.8	33.2	8.0	Sandy loam	1.56	0.41	8.41	8.03	111.70	8.15	7.0	98.9
20-120	65.3	26.7	8.0	Sandy loam	1.48	0.42	10.04	3.87	109.12	8.61	5.9	17.9
120-180	68.2	29.2	2.7	Sandy loam	1.45	0.45	7.45	1.52	87.60	8.66	6.3	20.2
180-200	32.0	51.0	17.0	Silt loam	1.25	0.51	0.66	5.41	161.80	8.27	4.4	19.0

Note: OC: Organic C; θ_s: Saturated water content, K_s : Saturated hydraulic conductivity, EC: Electric conductivity, pH: Potential of hydrogen, NH_4^+-N: Ammonia nitrogen, NO_3^--N: Nitrate nitrogen

Table 2. Irrigation (I) and fertilization (N, as urea) schedules for each treatment of the winter wheat during the experimental growing seasons. (units: mm for I and kg ha^{-1} for N)

Season	Treatment	Greening-Jointing		Jointing-Heading		Heading-Filling		Filling-Harvest		Total	
		I	N	I	N	I	N	I	N	I	N
2014	T1	20	105	80	–	–	–	–	–	100	105
	T2	20	315	80	–	–	–	–	–	100	315
	T3	80	105	–	–	–	–	80	–	160	105
	T4	80	315	–	–	–	–	80	–	160	315
	T5	80	210	80	–	–	–	80	–	240	210
2015	T1	20	105	–	–	80	–	–	–	100	105
	T2	20	315	–	–	80	–	–	–	100	315
	T3	80	105	–	–	–	–	80	–	160	105
	T4	80	315	–	–	–	–	80	–	160	315
	T5	80	210	–	–	80	–	80	–	240	210

Note: The T5 treatment represents conventional practice, and "–" shows no irrigation or fertilization applied.

Hydrol. Earth Syst. Sci. Discuss., https://doi.org/10.5194/hess-2018-234
Manuscript under review for journal Hydrol. Earth Syst. Sci.
Discussion started: 14 May 2018

Table 3. Evapotranspiration (ET) partitioning, grain yield, and water use efficiency (WUE) of the winter wheat under each treatment.

Season	Treatment	ET (mm)	T (mm)	E (mm)	T_{jf} (mm)	F_T (-)	Yield (kg ha^{-1})	WUE (kg ha^{-1} mm^{-1})
2014	T1	246.8	205.8	41.0	129.8	0.83	6493.2	26.3
	T2	258.4	208.9	49.5	130.9	0.81	6461.8	25.0
	T3	245.7	205.1	40.6	103.9	0.83	6026.0	24.5
	T4	295.6	247.7	47.9	144.5	0.84	7341.6	24.8
	T5	304.0	254.4	49.6	144.1	0.84	7276.8	23.9
	Mean	270.1	224.4	45.7	130.6	0.83	6719.9	24.9
	SD	27.7	24.5	4.5	16.5	0.01	569.2	0.9
2015	T1	281.3	206.2	75.1	136.0	0.73	7096.5	25.2
	T2	281.5	233.0	48.5	164.2	0.83	6965.5	24.7
	T3	308.7	261.9	46.8	162.1	0.85	6848.9	22.2
	T4	328.4	264.9	63.5	159.2	0.81	7044.5	21.5
	T5	377.3	297.3	80.0	205.8	0.79	6044.5	16.0
	Mean	315.4	252.7	62.8	165.5	0.80	6800.0	21.9
	SD	39.9	34.5	15.1	25.2	0.04	432.5	3.7

Note: T_{jf} means the sum of transpiration in jointing-heading and heading-filling periods, and F_T indicates the fraction of crop transpiration in evapotranspiration (T/ET).